forum acusticum 2026
8-12 September · Graz, Austria

PHYSICS-BASED MODELLING OF MECHANICAL IMPACT NOISE IN PIANO ACOUSTICS: HAMMER-STRING ACCELERATION NOISE

Pablo Miranda Valiente[1], Giacomo Squicciarini[1], David Thompson[1], David Owen Norris[2], Cesar Hernandez[3]

[1] *Institute of Sound and Vibration Research, University of Southampton, United Kingdom*
[2] *Music Department, University of Southampton, United Kingdom*
[3] *The Fortepiano Workshop, Swindon, United Kingdom*

This paper is a revised version of the authors' submitted manuscript that was peer-reviewed by at least two anonymous reviewers.

Abstract

This study examines a rarely considered acoustic consequence of the piano hammer–string collision: the direct sound produced by the hammer's rapid acceleration at impact. Using analytical methods and 2D finite element modelling, the resulting acoustic pressure is simulated and combined with the synthesised responses of a stiff string and soundboard radiation. The composite signal is analysed to assess the relative relevance of the impact-generated sound across the piano range. Results show that its contribution is generally minor, particularly for lower notes, and while typically masked under normal playing conditions, it may become noticeable in recordings with microphones placed near the action.

Keywords: *musical acoustics, piano acoustics, impact mechanics, collisions*

1. Introduction

The mechanical interactions between components of musical instruments are traditionally modelled using established methods such as Hertzian contact theory [1], penalty approaches in finite element analysis [2], and augmented Lagrangian techniques [3], with the primary aim of estimating contact forces and the resulting dynamics. In piano acoustics, collisions are typically examined to characterise the hammer–string interaction force [4], [5], [6], providing the forces that drive the motion of the piano's subsystems. In contrast, this study focuses on the sound produced directly by the large acceleration experienced by the hammer itself in the collision. The work is motivated by pianists' observations that the collision can generate a subtle, thud-like onset.

The mechanisms of impact noise have been classified by Akay [7] into several categories: air ejection, radiation due to rapid surface deformation, pseudo-steady-state radiation, material fracture radiation, and rigid-body radiation. The latter corresponds to a pressure disturbance in the surrounding fluid caused by the acceleration of an object, and has been studied extensively by Kirchhoff [8] and subsequent authors [9], [10], [11], [12], [13], [14]. In the context of piano acoustics, the hammer undergoes significant acceleration during contact with the string, and rigid-body radiation may be a relevant phenomenon on certain occasions.

This study models the acoustic pressure field generated by a sphere, undergoing an acceleration profile representative of the response to a hammer–string impact, used as an equivalent model for the hammer's rigid-body radiation. The approach is validated through comparison with 2D axisymmetric and 3D finite element models incorporating more realistic hammer geometries. The predicted impact-generated pressure is then combined with the output of a hammer–string–soundboard vibro-acoustic model to evaluate its relative significance within overall piano tone production.

2. NUMERICAL MODELLING

2.1. Analytical model

The sound radiated by a rigid piano hammer during its collision with a string is modelled as that produced by an equivalent sphere undergoing the same acceleration. Because the interaction occurs between the hammer and a string rather than with a surface, the radiating body is assumed to be this equivalent sphere. This contrasts with studies involving surface impacts, where

Corresponding author: *P.M.Miranda-Valiente@soton.ac.uk.*

an image source must be introduced to account for the reflection [11]. Consider a sphere impacting a thin string-like surface as in Fig. 1.

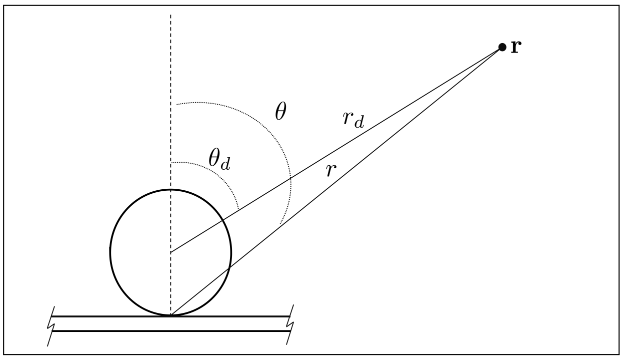

Figure 1: Sphere impacting on string-like surface.

Developed originally by Kirchhoff [8], the pressure radiated by a sphere with radius a undergoing unit acceleration, at a point $\mathbf{r}$ located at (r, θ) is [11]

$$p_{acc}(r,\theta,t') = \rho_0 c \frac{a^2}{r^2} \left[\left(1 - \frac{r}{a}\right) \sin \frac{c}{a} t' + \frac{r}{a} \cos \frac{c}{a} t' \right] e^{-ct'/a} \cos\theta \tag{1}$$

where ρ_0 and c are the density and sound speed of the fluid in which the sphere is immersed and $t' = t - (r-a)/c$ is the retarded time. If an arbitrary acceleration $A(t)$ is applied to the sphere, the resultant acoustic pressure is given by the convolution integral:

$$p(t) = \int_0^t p_{acc}(r,\theta,t-\xi)A(\xi)d\xi \tag{2}$$

2.2. Finite-element model

It is necessary to adapt the analytical model to consider the geometry of the piano hammer, thus a two-step verification method is applied. Firstly, the analytical model is compared with a corresponding 2D axisymmetric FE model, and secondly, a full 3D model is developed to consider the exact hammer shape. The first step ensures an adequate implementation of the FE model setup, while the 3D model allows the analytical model to be tuned to produce an equivalent acoustic pressure. The FE models are developed in COMSOL Multiphysics® v.6.4[15].

2.2.1. 2D axisymmetric FE model

A 2D axisymmetric model is developed, making use of the axisymmetry of the sphere. The surrounding fluid is modelled as a sphere with a radius of 3 m enclosed in a perfectly-matched layer (PML) of a thickness of 1 m, to avoid unwanted reflections from the outer boundary of the model. Ten (10) elements per wavelength considering a maximum frequency of 1000 Hz, are used in the mesh (see Fig. 2) yielding ≈ 58500 degrees of freedom (DoF).

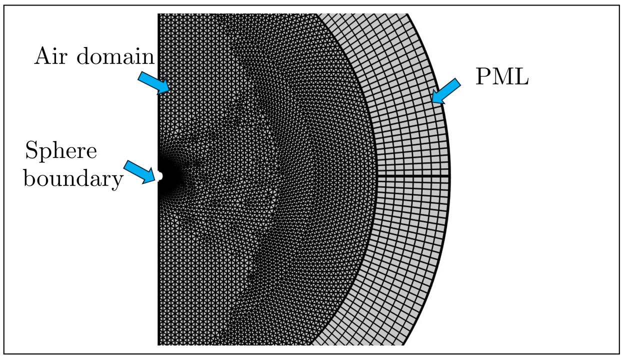

Figure 2: Mesh of 2D axisymmetric model.

2.2.2. 3D FE model

The real hammer geometry is not axisymmetric, thus a 3D model is needed. To avoid excessive computational expense, the air domain and the PML thickness were reduced to a sphere of 0.5 m and a PML thickness of 0.15 m. The model now considers ≈ 236000 DoF. The meshed model is shown in Fig. 3, where the 3D geometry of the hammer is highlighted.

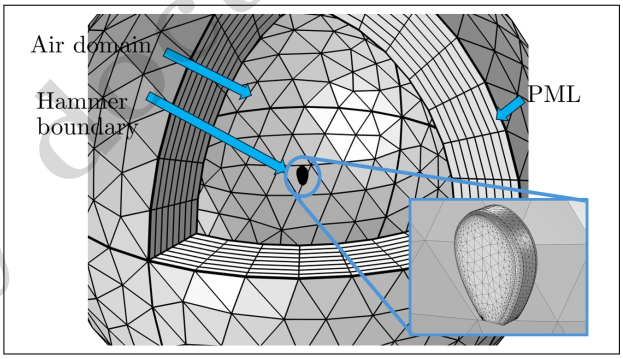

Figure 3: Mesh of 3D model.

2.3. Hammer-string-soundboard model

A time-domain state-space modal model, previously adopted by the authors [16], is used to represent the transverse interaction—perpendicular to the soundboard—between the hammer and the string. This model is used first to determine the acceleration experienced by the piano hammer, which serves as input to the collision-induced acoustic pressure model, and second to evaluate the force transmitted to the soundboard and the resulting sound radiation. Consequently, the modelling framework adopted in this study enables a clear distinction between the acoustic pressure generated by the hammer–string collision and that produced by the radiation of the piano soundboard. The state space equations are

$$\begin{aligned} \dot{\mathbf{x}} &= \mathbf{A}\mathbf{x} + \mathbf{B}F_H \\ \mathbf{y} &= \mathbf{D}\mathbf{x} \end{aligned} \tag{3}$$

where the state vector is $\mathbf{x} = \{\mathbf{q}^T, \dot{\mathbf{q}}^T, y_H, \dot{y}_H\}^T$ containing the modal coordinates of the string $\mathbf{q}$ and the displacement and velocity of the piano hammer y_H and $\dot{y}_H$. The state-space matrix $\mathbf{A}$ contains the modal damping and stiffness matrix of the string, and the matrix $\mathbf{B}$ transforms the hammer force F_H to a modal force, and contains the mode shapes of the simply supported string at the excitation point. The force applied to the hammer is given by the power law [4]

$$F_H = K_H \delta^p \tag{4}$$

where K_H is the nonlinear stiffness of the hammer, δ is the compression of the hammer felt and p is the nonlinear exponent representing the nonlinear behaviour of the compression. The acceleration of the hammer during the contact is simply

$$A(t) = F_H / m_H \tag{5}$$

The string is modelled as a simply supported string of length L, and the force applied to the soundboard at the bridge is given by

$$F_\mathbf{b} = -T \left.\frac{\partial v}{\partial x}\right|_{x=L} \tag{6}$$

where T is the tension of the string and v its transverse displacement.
A generic soundboard is developed in COMSOL Multiphysics. The soundboard is discretised in a fine grid of points and its transfer mobility response $\mathbf{Y}(\omega)$ is computed. To obtain the sound pressure at a receiver, the Rayleigh integral method is used in matrix form to obtain the pressure-to-force ratio

$$\frac{P(\omega)}{F_\mathbf{b}(\omega)} = \mathbf{M}(\omega)\mathbf{Y}(\omega) \tag{7}$$

where $\mathbf{M}(\omega)$ is the radiation impedance matrix computed at the receiver point.
The total acoustic pressure at a receiver position $\mathbf{r}$ considering the soundboard radiation and the rigid body radiation of the hammer is given by

$$P_{tot}(t) = \mathrm{IFFT}(P_\omega) + p(t) \tag{8}$$

3. RESULTS

In this section the modelling results are presented. First, the analytical model is verified with the simple 2D axisymmetric model. Subsequently, the analytical model is compared with a 3D FE model that considers the geometry of a piano hammer.

3.1. Verification of analytical model

To verify the implementation of the analytical model against the FE model a simple excitation consisting in a half-cosine of maximum amplitude A_0 and duration τ is used, which can be written as

$$A(t) = \begin{cases} A_0(-\cos^2(\pi t/\tau) + 1), & \text{if } t \leq \tau \\ 0, & \text{otherwise} \end{cases} \tag{9}$$

The acoustic pressure provided by the analytical model is compared to that obtained from the 2D axisymmetric model. The parameters used in the verification are presented in Table 1. In the FE model the same parameters are used.

Table 1: Parameters for verification of analytical model.

Description	Variable	Unit	Value
Air density	ρ_0	kg/m^3	1.2
Sound speed in air	c	m/s	343
Radius of sphere	a	m	0.035
Receiver distance	r	m	0.5
Accel. amplitude	A_0	m/s^2	1
Time step	dt	s	5×10^{-7}
Sampling frequency	f_s	Hz	2×10^6
Calculation duration	t_{max}	s	0.008
Duration of contact	τ	s	0.015

Calculations are developed for different angles θ_d (see Fig. 1): 0°, 30°, 60° and 80°. The results are shown in Fig. 4, there is good agreement between the computed acoustic pressures for different angles, however near the shadow zone of the acoustic dipole, i.e., at 80° the agreement is reduced. This implies that the models produce an acoustic-like dipole that differs in directivity. Differences in the maximum A-weighted fast sound level ($L_{AF\max}$) were calculated and are shown in Table 2, evidencing that the analytical model is capable of effectively representing the acoustic pressure of an accelerating sphere, within 60°.

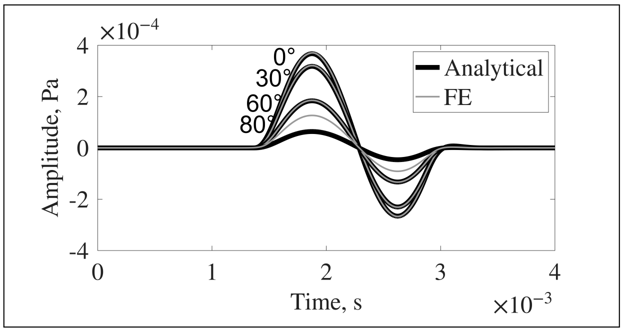

Figure 4: Comparison between the acoustic pressure from analytical model and FE model for different θ_d.

To verify the decay of the pressure at different distances, the pressure is calculated over distances $r_1 = 0.125$ m, 0.25 m, 0.5 m, 1 m, using $\theta_d = 30°$. The comparison between the analytical and the FE model is shown in Fig. 5, where a good agreement can be observed for the differences studied.

Table 2: Difference in fast, A-weighted maximum sound level between analytical and FE models for different angles θ_d.

θ, degrees	$\Delta L_{AF\max}$, dB
0	0.1
30	0.1
60	0.1
80	5.9

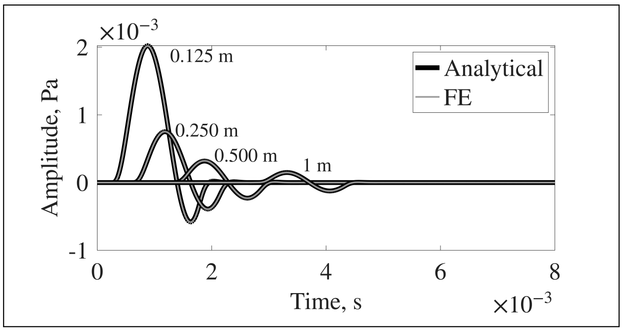

Figure 5: Comparison between the acoustic pressure from analytical model and FE model for different distances.

Differences in $L_{AF\max}$ are shown for different distances in Fig. 5, indicating that there are no significant differences.

Table 3: Difference in fast, A-weighted maximum sound level between analytical and FE models for different distances.

r_1, m	$\Delta L_{AF\max}$, dB
0.125	0
0.250	0
0.500	0.1
1.0	0

3.2. Analytical model compared to 3D FE model

To evaluate the applicability of the analytical model for representing the piano hammer, the hammer has been measured and is modelled in COMSOL using its CAD tools. An equivalent sphere with the same volume as the modelled hammer is then used within the analytical framework to approximate its physical characteristics. In both models a distance of $r_d = 0.125$ m and an angle of $\theta_d = 30°$ were used for comparison. The same distances and angles are used in both models for these comparisons. The difference in $L_{AF\max}$ is ≈ 2 dB. To improve the agreement between the analytical and FE models—acknowledging that their geometries are not identical—a scaling factor of 0.84 is applied to the analytical sphere volume. This adjustment provides the best match to the FE model, achieving a maximum pressure difference of $\Delta L_{AF\max} = 0.1$ dB.

However, as was shown in Section 3.1, the agreement is decreased closer to the shadow zone of the dipole, thus the scaling factor would need to be adjusted accordingly. The comparison between the unmodified analytical model, its modified version and the FE model is shown in Fig. 6.

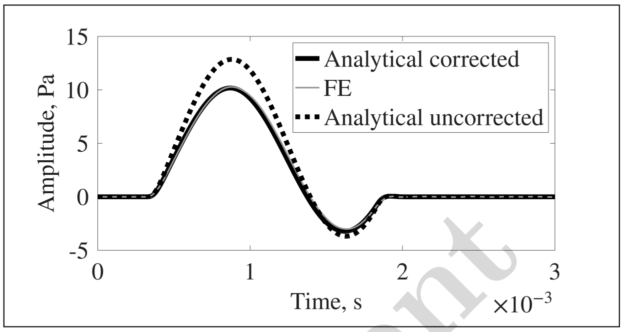

Figure 6: Comparison between the acoustic pressure at $r_d = 0.125$ m from analytical model and FE model of a piano hammer.

3.3. Combined pressure

The acoustic pressure resulting from different accelerations corresponding to various piano touches and for two example notes, C2 and C7, is combined with the radiated pressure from the soundboard originating from the string vibration model. The coordinate system is shown in Fig. 7, highlighting the location of the hammer collision $\mathbf{r}_H$ (in plane with the soundboard), the location of the receiver $\mathbf{r}_r$, and the location of the connection point between the two strings analysed and the soundboard where the force $F_\mathbf{b}$ is applied to the soundboard.

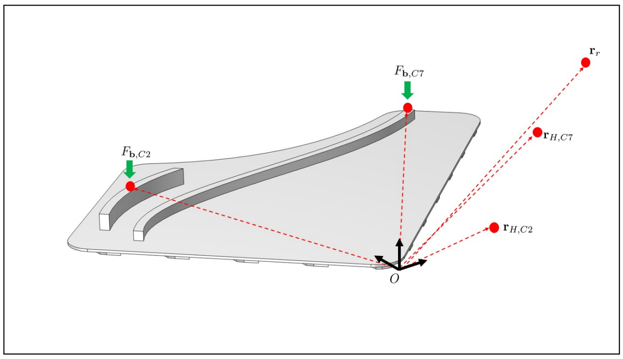

Figure 7: Coordinate system used for calculation of pressure at the receiver $\mathbf{r}_r$.

The time-domain state-space model is solved using the physical parameters of a measured C2 string and the hammer properties reported by Chaigne and Askenfelt [17]. To capture the full decay of the string, the response is computed over a duration of 15 s with a sampling frequency of 44.1 kHz. The spectra of the forces are multiplied by the pressure to force ratio to yield the acoustic pressure at the receiver point radiated by the soundboard.

From the different accelerations obtained from the various collisions using the range of hammer impact velocities $\dot{y}_{H,t=0} = 1, 2, 4, 6, 8, 10$ m/s, the acoustic pressure associated with the rigid body radiation of the piano hammer is calculated at the receiver location $\mathbf{r}_r$, and shown in Fig. 8.

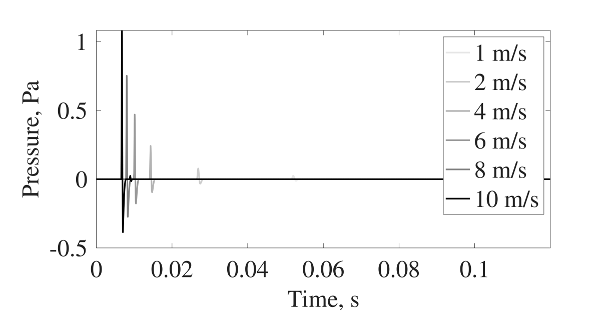

Figure 8: Time history of acoustic pressures due to hammer-string collision for different hammer impact velocities.

Summing the collision pressures with the soundboard radiation produces an amplitude of max 3–3.5 Pa as shown in Fig. 9; the acceleration-noise signature is entirely masked.

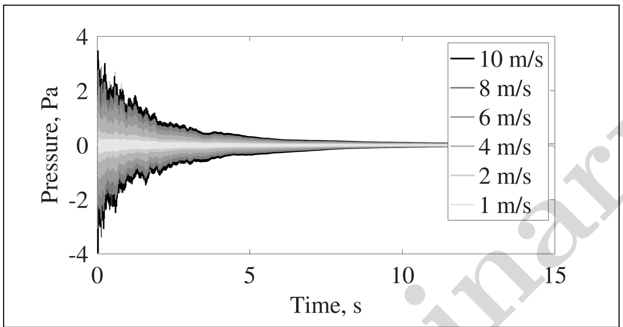

Figure 9: Time histories of the combined pressures for different hammer impact velocities.

The spectra of the combined pressures are shown in Fig. 10, where the sound pressures obtained without the collision are also included. For this note, the contribution of impact sound is negligible. The time-history of the total radiated sound, as well as informal listening tests, confirms that the impact components are not perceptually distinguishable.
As shown in Fig. 11, the influence of collision-generated pressure increases in the higher register. For the C7 string, the weaker forces transmitted to the soundboard produce lower radiated sound levels than in the C2 case, making the collision contribution more noticeable at low frequencies. Time-domain results and informal listening suggest that, for C7, this manifests as a subtle popping-like onset. There is no influence on the inharmonic partials of the string, as the resonance at 2093.7 Hz remains unaltered. The relative levels of combined

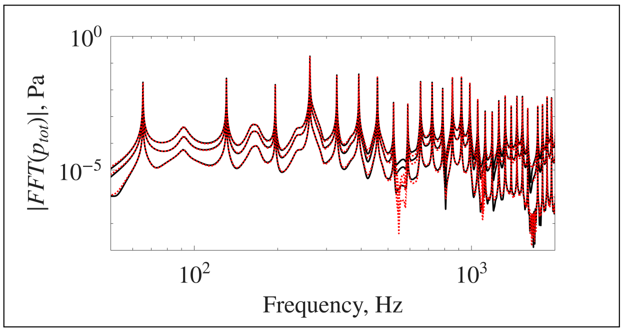

Figure 10: Pressure spectra of combined pressures (black line), and only soundboard radiation (dotted red line) for different hammer impact velocities: 1, 4 and 8 m/s.

and soundboard-radiated pressures for different hammer speeds (1, 4, and 8 m/s) are illustrated in Fig. 12.

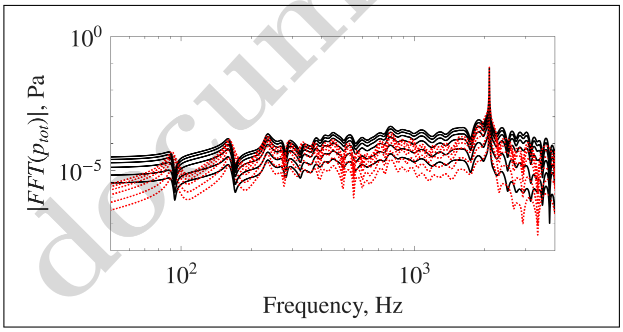

Figure 11: Pressure spectra of combined pressures (black line), and only soundboard radiation (dotted red line) for different hammer impact velocities, for the C7 case

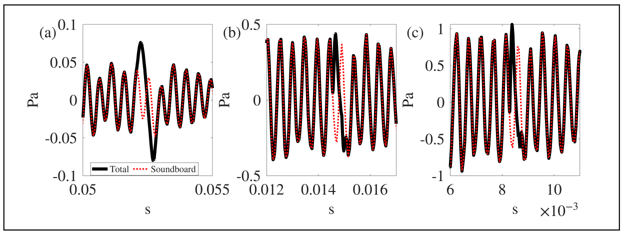

Figure 12: Time histories of combined pressures (black line), and only soundboard radiation (dotted red line) for hammer impact velocities (a) 1 m/s, (b) 4 m/s and (c) 8 m/s, for the C7 case.

To highlight the positional dependence of the collision-generated pressure, three receiver locations were tested at increasing proximity to the hammer–string impact point $\mathbf{r}_{H,C7}$. As shown in Fig. 13, receiver 1 follows the configuration of Fig. 7, while receivers 2 and 3 are placed 40 cm and 20 cm in front of $\mathbf{r}_{H,C7}$, respectively. Using the largest impact velocity (10 m/s), the spectra show that moving the receiver closer to the impact point increases the difference between the combined and soundboard-radiated pressures, particularly below 100 Hz and in the 1–2 kHz region.

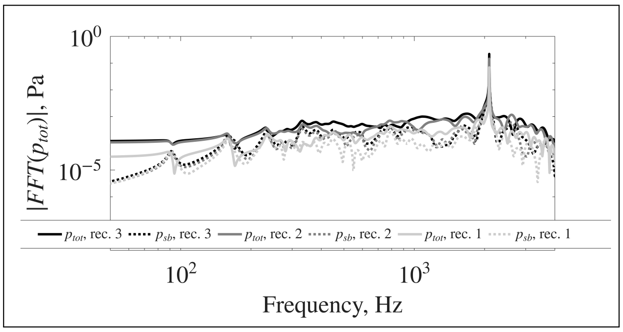

Figure 13: Pressure spectra of combined pressures (solid), and only soundboard radiation (dotted line) for different receivers, for C7 case

Physical phenomena such as longitudinal vibrations or hammer shank flexibility could be included in a more complete model. However, longitudinal vibrations are more important for low notes, and shank flexibility has a small effect on force transmission, but can produce smaller contact forces[18], thus smaller accelerations.

4. Conclusions

The hammer–string collision was modelled using an analytical impact formulation and validated against finite element simulations, showing good agreement. The results indicate that collision-generated acoustic pressure is negligible in the low register but can contribute measurably at higher notes, especially for receivers or microphones placed close to the hammer. While this mechanism may enhance realism in sound synthesis, further experimental validation and additional physical effects need to be included to fully assess its significance.

5. Acknowledgments

The research conducted by the authors was funded by the Leverhulme Trust (Grant Ref: RPG-2024-426).

References

[1] H. Hertz, “On the contact of rigid elastic solids and on hardness,” in *Miscellaneous Papers*, P. Lenard, Ed. London: Macmillan, 1896, ch. VI, pp. 163–183.

[2] A. Francavilla and O. C. Zienkiewicz, “A note on numerical computation of elastic contact problems,” *International Journal for Numerical Methods in Engineering*, vol. 9, no. 4, pp. 913–924, 1975.

[3] P. Wriggers, “Penalty and augmented lagrangian formulations for contact problems,” in *NUMETA 85*, Swansea, UK, Jan. 1985.

[4] M. Ghosh, “An experimental study of the duration of contact of an elastic hammer striking a damped pianoforte string,” *The Indian Journal of Physics*, vol. 7, pp. 365–382, 1932.

[5] K. Hunt and E. Crossley, “Coefficient of restitution interpreted as damping in vibroimpact,” *Journal of Applied Mechanics*, 1975.

[6] A. Stulov, “Hysteretic model of the grand piano hammer felt,” *The Journal of the Acoustical Society of America*, vol. 97, no. 4, 1995.

[7] A. Akay, “A review of impact noise,” *The Journal of the Acoustical Society of America*, vol. 64, no. 4, pp. 977–987, Oct. 1978.

[8] G. R. Kirchhoff, *Vorlesungen über mathematische Physik. Band 1: Mechanik*, Dritte Auflage. Leipzig: B. G. Teubner, 1883, pp. 316–320.

[9] M. C. Junger and W. Thompson Jr., “Oscillatory acoustic transients radiated by impulsively accelerated bodies,” *The Journal of the Acoustical Society of America*, vol. 38, no. 6, pp. 978–986, Dec. 1965.

[10] L. Koss and R. Alfredson, “Transient sound radiated by spheres undergoing an elastic collision,” *Journal of Sound and Vibration*, vol. 27, no. 1, pp. 59–75, 1973.

[11] A. Akay and T. H. Hodgson, “Acoustic radiation from the elastic impact of a sphere with a slab,” *Applied Acoustics*, vol. 11, no. 4, pp. 285–304, 1978.

[12] E. J. Richards, M. E. Westcott, and R. K. Jeyapalan, “On the prediction of impact noise, i: Acceleration noise,” *Journal of Sound and Vibration*, vol. 62, pp. 547–575, 1979.

[13] K. G. Manoj and S. K. Bhattacharyya, “Transient acoustic radiation from impulsively accelerated bodies by the finite element method,” *The Journal of the Acoustical Society of America*, vol. 107, no. 3, pp. 1179–1188, Mar. 2000.

[14] J. N. Chadwick, C. Zheng, and D. L. James, “Precomputed acceleration noise for improved rigid-body sound,” *ACM Trans. Graph.*, vol. 31, no. 4, Jul. 2012.

[15] COMSOL Inc., *Acoustics Module User’s Guide*, COMSOL Multiphysics® v. 6.4, Stockholm, Sweden: COMSOL AB, 2025.

[16] P. M. Valiente, G. Squicciarini, and D. Thompson, “Influence of soundboard modelling approaches on piano string vibration,” *The Journal of the Acoustical Society of America*, vol. 155, no. 5, pp. 3213–3232, 2024.

[17] A. Chaigne and A. Askenfelt, “Numerical simulations of piano strings. ii. comparisons with measurements and systematic exploration of some hammer-string parameters,” *The Journal of the Acoustical Society of America*, vol. 95, no. 2, 1994.

[18] P. M. Valiente, “Modelling of sound generation in pianos,” Ph.D. dissertation, University of Southampton, 2025. [Online]. Available: `https://eprints.soton.ac.uk/504922/`.